1-1-2020

Development Of An Ophthalmic Nanoemulsion Topical Formulation For Corneal Wound Healing

Chuntian Cai

DESIGN AND DEVELOPMENT OF AN OPHTHALMIC NANOEMULSION TOPICAL FORMULATION FOR CORNEAL WOUND HEALING

A Thesis

Presented for the degree of

The Master of science in Pharmaceutical Sciences

with Emphasis in Pharmaceutics and Drug Delivery

By

Chuntian Cai

Department of Pharmaceutics and Drug

Delivery School of Pharmacy

The University of Mississippi

205, Faser Hall, School of Pharmacy, Oxford, MS

(May, 2020)

ABSTRACT

Corneal wound healing is a complex process involving cell death, migration, proliferation, differentiation, extracellular matrix remodeling and a various of growth factors. Of these factors, interleukin-1 and transforming growth factor beta allow the effectiveness of cell migration and tissue repair. Current management advocates multiple therapies aimed to prevent inflammation, avoid the fibrosis. Pirfenidone (PFD) has recently been investigated for its anti-fibrotic effect. The current study was undertaken to develop and optimize PFD-loaded nanoemulsion (NE; PFD-NE) which could increase the drug load and the duration of activity. Hot homogenization and probe sonication methods were used for the preparation of PFD-NEs, sesame oil and soybean oil as the oil part, Tween 80 and Poloxamer 188 as surfactants. Physicochemical properties of PFD-NE formulations were characterized such as particle size, polydispersity index, zeta potential and assay. The physical and chemical stability of the optimized PFD-NEs were observed under refrigerated and room temperature for one month. PFD-NE formulations showed desirable physical properties and observed to be stable for one month. Furthermore, in-vitro release studies of optimized PFD-NE formulations were performed in comparison with PFD solution (PFD-C) as control. From the release studies, a sustained release of the PFD was observed in PFD-NE formulations compared to PFD-C. Generally, the PFD-NE formulations showed great potential as an alternative delivery system for corneal wound healing treatment.

ACKNOWLEDGMENTS

This thesis is dedicated to those who supported me in my own times of stress and anxiety. I would like to thank Dr. Soumyajit Majumdar and all the other members of my lab for their wonderful patience, warm humor and continued support. I would like to thank Corinne Sweeney for her practical help, and my postdoctoral, Dr. Narendar Reddy for his advice and trust in me.

LIST OF ABBREVIATIONS AND SYMBOLS

Pirfenidone: PFD

Nanoemulsion: NE

Polydispersity Index: PDI

Zeta Potential: ZP

High-pressure liquid chromatography: HPLC

Poloxamer 188: P188

Tween®80: T80

Food and drug administration: FDA

Inactive Ingredients Guide: IIG

Percent weight per weight: % w/w

Percent weight per volume: % w/v

Revolutions per minutes: RPM

Millimeter: mm

Microliter: µL

Milliliter: mL

Standard deviation: SD

Nanometer: nm

Percent relative standard deviation: % RSD

Acetonitrile: CAN

Limit of detection: LOD

Limit of quantification: LOQ

Table of Contents

List of Figures

List of Tables

Chapter 1 Introduction

1.1 Anatomy of the Cornea

Cornea is part of the eye which is exposed to the outside environment and is therefore most likely to suffer harm due to various threats. Since light enters the eye first, the cornea provides refractive power which helps to focus light rays on the retina. Therefore, the cornea is a key component of the refractive ocular system. It is a translucent and avascular tissue. The human cornea consists of five membranes. It includes three cellular layers (epithelium, stroma, endothelium) and two interface layers (Bowman membrane, Descemet membrane). Corneal curvature and transparency are essential to maintain the corneal refractive force, which accounts for about 2/3 of the eye's refractive power. The horizontal diameter of the cornea is 11.5-12.0 mm in the average adult and the vertical diameter is smaller by approximately 1.0 mm.[1] Corneal form and curvature are regulated by its intrinsic biomechanical structure and the extrinsic environment.

1.2 Epithelium wound healing

The epithelium is the outermost layer of the cornea. It is the first barrier to the outside and is an integral part of the film-corneal interface which is important for the

refractive ocular system. Corneal epithelium is a self-generating tissue with stem cell residue in the corneoscleral junction, limbus, and providing proliferating cells for epithelial regeneration.[2] The epithelium wound healing is a dynamic process to maintain the integrity and protection of the corneal epithelial surface to maintain corneal consistency and vision. The repairing of corneal epithelial wounds includes cell migration, proliferation, adhesion and cell layer stratification.[3]

After injury, at the wound site, an intrinsic cascade involving growth factor/cytokine and extracellular matrix (ECM) signal-mediated interactions between epithelial cells, stromal keratocytes, and cells of the immune system control this process, influencing the expression of matrix metalloproteinases (MMPs). In physiological conditions, MMPs catalyze ECM molecules, such as collagen, proteoglycans, and fibronectin, maintaining the structure and functions of the cornea.[4] Growth factors (GFs) and cytokines such as interleukin-1 (IL-1) and transforming growth factor-β (TGF-β), allow the effectiveness of cell migration and tissue repair, regulate the expression of MMPs. Epithelial cells evoke sequential steps attempting to re-establish epithelial integrity and restore corneal homeostasis, eventually sealing the wound.[5]

1.3 The role of GFs and cytokines in epithelial wound healing

GFs and cytokines regulate the growth, proliferation, migration, differentiation, ECM deposition of the cells involved in wound healing. GFs and cytokines play an important role in mediating different cell functions with intracellular and intercellular signaling molecules.[6] During wound healing, corneal cells express many GFs and cytokines which have specific effects on epithelial cells, such as epidermal GF (EGF),

platelet-derived GF(PDGF) and TGF-α, TGF- β, IL-1, IL-6, IL-10, and tumor necrosis factor (TNF)-α. Such cellular interactions are not exclusive, and some activities can base on or mediate other factors.

1.4 EGF family

EGF signaling comprises a major pathway that initiates cell migration and proliferation and stimulates corneal epithelial wound healing. The EGF family is composed of up to 13 members and the main members involved in epithelial wound healing include EGF, TGF-α. The level and function of the EGFR are essential determinants for the epithelial cell condition in tissues and organs, so maintaining a sufficient level of EGFR signaling is important for corneal homeostasis. During wound healing, TGF-α are increased while EGF and mRNA levels remain unchanged, which indicates EGF maybe indirectly involved in stimulating epithelial wound closure.[3] A few hours after an epithelial injury or corneal inflammation, monocytes, granulocytes, T-cells and other immune cells migrate to the corneal stroma. When this occurs, the IL-1 and TNF-α released by epithelial that leading to epithelial cell migration by activating a variety of responses through ERK, MAP kinases, and/or NF-κB pathway, then induces the production of monocyte chemotactic stimulant and granulocyte colony-stimulant hormone through keratocytes, attracting the inflammatory cells to stroma. [7-9]

1.5 TGF-β

The isoforms TGF-β, TGF-β1, TGF-β2 and TGF-β3 are expressed in corneal epithelium, stromal keratocytes and tear fluids with TGF-β2 expressed at higher levels.[10] TGF-β1 and TGF-β2 inhibit corneal epithelial cell proliferation *in vitro* while

TGF-β3 mediate the binding of other TGF isoforms and further regulate the receptor activities by the co-receptors endoglin and betaglycan.[11] When inactive precursors attached to latency-associated peptides TGF ligands are either activated or integrated into the extracellular matrix (ECM) to be activated later. Epithelial wound healing occurs in a phased process with specific physiological functions. TGF-β stimulates the migration of corneal epithelial cell via integrin β1, which mediates p38 MAP kinase activation, ECM expression.[12, 13] The p38 MAP kinase delayed the initiation via the main TGF-β SMAD signaling pathway or by an alternate c-Jun N-terminal kinase (JNK) pathway.[14]

1.6 Corneal Stromal Wound Healing

Corneal stromal wounds are common. The response of the corneal wound to stromal damage requires a sequence of events which would return to normal stromal structure and function.[15] After an epithelial injury, keratocyte death by apoptosis occurs in the central stroma. The injury-induced keratocyte apoptosis allows cytokines such as Fas ligand, IL-1, and TNF-α to release out of epithelial cells and/or tears.[16] These cytokines cause rapid apoptosis by Fas/Fas ligand system. More specifically, IL-1 induces keratocytes to generate Fas ligand RNA and protein to activate apoptotic autocrine response. Thus, when stimulated by IL-1, both Fas ligand and Fas are produced, and this simultaneous expression triggers apoptosis via autocrine mechanisms.[17] The stromal apoptosis process typically lasts several days to a week after the injury. This period also involves the death of inflammatory cells and other bone marrow-derived cells like myofibroblast precursor cells, which enter the stream of the limbal vessels immediately. Then, the dying cells in the stroma undergo necrosis.

1.7 Myofibroblast transdifferentiation in stromal wound healing

Myofibroblasts, sometimes referred to as being 'activated' fibroblastic cells, is considered as a critical factor leading to opacity or fibrosis of the cornea.[18] After corneal epithelial injury, usually 12-24 hours, residual activated keratocytes proliferate and migrate in the peripheral and posterior stroma change their properties to become myofibroblast at the wound edges until they completely fill the wound. Excessive quantities of ECM proteins, including collagen and fibronectin, which distort normal corneal organization ECM deposit and cross-link,[19] cause the abnormal corneal curvature and refractive error.

In culture, some growth factors (FGF-2 and PDGF-AB, TGF-β) mediate this process, while others (IL-1 and IGF-1) confer only mitogenic activity.[20] The activated stromal keratocytes (also known as stromal fibroblasts) inhibit the expression of differentiated keratocyte proteins and begin producing proteinases (usually MMPs) required to reshape the wound ECM. After entering the wound site, fibroblasts start to express α-smooth muscle actin (α-SMA) and desmin, upregulate the expression of vimentin and become highly mobile and contractile myofibroblasts necessary for wound reconstruction of ECM and wound contraction **(**Fig 1). These fibroblasts deposit temporary ECM rich in fibronectin and some other proteins, including tenascin-C and collagen type III. Myofibroblasts provide contractile forces to close a wound space, and (α -SMA) expressions directly correlate with the contraction of corneal wound.[21] When wound healing is complete, upregulation of IL-1 produced by stromal cells triggers the apoptosis of the myofibroblasts and deprives them of TGF-β.[5] Then keratocytes reoccupy the anterior stroma, absorb the abnormal ECM

proteins, restore corneal integrity and transparency. During this process, persistent release of TGF-β leads to the maintenance of the myofibroblasts that continue to secrete and deposit anomalous ECM, eventually causing corneal haze.

Fibrotic and scarring processes are mainly driven by the proliferation of fibroblasts and exuberant ECM expression. It was shown that fibroblasts from different ocular tissues differ in their mRNA profiles.[22] Many signaling pathways, including the (PI3K)/AKT pathway, extracellular signal regulated kinase (ERK)/mitogen-activated protein kinase (MAPK), c-Jun N-terminal kinase (JNK)/MAPK, and p38MAPK pathways, participate in the fibrosis process and impact fibroblast proliferation.[14, 23]

Currently, there is no treatment for the eradication of scar tissue, and the conventional strategy of wound healing modulation is to prevent infections, reduce inflammation, so as to prevent and avoid the formation of a scar, while ensuring optimal conjunctival wound healing. One of the wound healing regulations covers all steps taken against inflammatory cell proliferation and activation. Thus, topical corticosteroid is an essential part. However, topical ophthalmic corticosteroid use can result in complications such as intraocular pressure (IOP) elevations, posterior subcapsular cataract formation with long-term use, secondary infection, and delays in corneal wound healing.[24] Another therapeutic choice is the application of the antimetabolite mitomycin C (MMC) as a prophylactic after Photorefractive Keratectomy (PRK) for high myopia. However, due to its antimitotic function, MMC-induced apoptosis of inactive keratocytes has acute cytotoxicity adverse effects such as necrosis, and could be related to long-term adverse effects such as corneal thinning.[25] Such difficulties underscore a need to develop effective, safe, and well-tolerated agents which can modulate the wound healing.

PFD (5-methyl-1-phenyl-2-[1H]-pyridone) is a novel compound which shows anti-fibrotic and anti-inflammatory effects in organs such as the lung [26-29], the liver [27]and the kidney.[30] The PFD is a small molecule (molecule weight ≈185g/mol) with amphiphilic solubility(log D of 1.37 ±0.05).[31][need to include what is know about the physical-chemical properties of the drug including water solubility, Log P, and stability] In United States, the Food and Drug Administration approved oral PFD for the treatment of idiopathic pulmonary fibrosis (IPF) in 2014. Recently, several studies reported the use of PFD in ocular tissues, PFD inhibited human Tenon`s fibroblasts` (HTFs) proliferation and biological activity *in vitro.*[32] The mechanisms could be act as by inhibiting mRNA and protein expression of transforming growth factor-β (TGF-β) isoforms.[33] Also, PFD regulates a series of cytokines such as inflammatory cytokines TNFα and IL-1.[34] Additionally, PFD arrested the cell cycle by downregulating CDK6/cyclin D and CDK2/cyclin E which involved the inhibition of the AKT/GSK3b, ERK/MAPK, and JNK/MAPK signaling pathways while activated the p38 MAPK signaling pathway.[23] In the eye, PFD has shown the prevention of corneal scarring, and the inhibition of orbital fibroblasts migration, the anti-fibrotic influence is primarily due to its antagonism of fibroblast proliferation and migration and the reduction of matrix deposits of ECM.[32] However, when the PFD topically administered as 0.5% w/v eye drop in rabbit eyes, the pharmacokinetics of PFD exhibited a shorter half-life in cornea tissue (less than 19 min) as expected for ophthalmic formulations.[35]

The topical administration is the most common ophthalmic dosage form as it is non-invasive, low cost and easy to use. However, poor ocular drug bioavailability is one of the most difficult areas for researchers to deal with due to the eye's complex anatomy, physiology and biochemistry.[36] Most drugs administered on the ocular

surface from solutions are rapidly drained by different mechanisms, such as blinking, tearing and tear dilution. Tear turnover from lacrimal secretions lead to a majority loss of the drug. The tear volume of a healthy eye is ~7–9 μL, and its turnover rate is 0.5–2.2 μL/min.[37] The average volume of major formulations during topical administration is ~35–56 μL, and the excess volume drains into systemic circulation through the nasolacrimal duct. It is estimated that 5% or even less of the dose administered enters intraocular devices.[38] To improve ocular bioavailability, various ophthalmic drug delivery systems, emulsions, nanoparticles and suspensions [39-41] have been proposed. These systems can improve the bioavailability of the drugs facilitating transcorneal/transconjunctival penetration.

Nanoemulsion (NE) formulations are thermodynamically and kinetically stable isotropic distributions, composed of multi-component fluids, and usually consist of an aqueous phase an oil phase, stabilized with a single phase interfacial layer composed of an primary surfactant as an emulsifying agent, a cosurfactant usually an alkanol of intermediate chain length and occasionally an electrolyte.[42] The major benefits of the NE formulation involve sustained release of the drug administered to the cornea, high penetration into the deep layers of the ocular tissue, aqueous humor and ease of sterilization. Therefore, these processes may have lower dosage and less systemic and ocular side effects.

Chapter 2 Materials and Methods

2.1 Materials

PFD was purchased from Fisher Scientific (TCI America, USA). Castor oil NF grade, Poloxamer 188, Sesame oil NF grade, Soybean oil NF grade and Tween® 80 (T80) (polysorbate 80) NF grade were purchased from Spectrum Pharmaceuticals (Henderson, NV). All other chemicals were purchased from Fisher Scientific (St. Louis, MO, USA). Solvents used for analysis were of High-Performance Liquid Chromatography (HPLC) grade.

2.2 Methods

2.2.1 HPLC method development

PFD were analyzed using an HPLC-Ultraviolet system comprising a Waters 717 plus autosampler, Waters 600E pump controller, Waters 2487 dual λ Absorbance detector. Stock solutions of PFD were prepared in acetonitrile (ACN). A mobile phase consisting of 80:20 ACN and Millipore water was used on a Phenomenex® C_{18} (4.6 x 250 mm, 5 microns) column at a flow rate of 1.0 mL/min. The samples were detected at a wavelength of 314 nm and a runtime of 7 minutes. Each injection volume was 20 µL. The method was validated in accuracy, precision. linearity, LOD and LOQ according to the guidelines issued by the FDA. The summary of the HPLC method shown in Table 1.

Table 1 Summary of HPLC analytical method of PFD

Mobile Phase	80% ACN: 20% Millipore water
Column	Phenomenex Luna® C_{18} (250x4.6mm,5µm)
Flow rate	1.0 mL/min
Detector	UV
Wavelength	314 nm
Column temperature	Room temperature
Solvent delivery module	Waters 600
Data processor	Waters 717 plus Auto sampler
Sensitivity	2.0 AUFS
Retention Time	3.5 ± 0.1mins
Linearity (R^2)	0.9995
LOD	0.1µg/mL
LOQ	0.25 µg/mL
Precision	% RSD (1.04-2.37)
Accuracy	% RSD (0.12-2.24)

2.2.2 Screening of Oil

Screening of different oils were carried out based on our previous lab work.[43] Three oils were screened based on concentrations disclosed in the Food and Drug Administration (FDA) Inactive Ingredients Guide (IIG) for ophthalmic or parenteral use.[44] Castor oil is contained in IIG ophthalmic formulations at a concentration of 0.15% w/v. Sesame oil is contained in IIG approved intramuscular emulsion

formulations at a concentration of 70% w/v. Soybean oil is contained in IIG intravenous emulsion formulations at a concentration of 20% w/v. NE placebo formulations were made using the oil concentrations (5% w/v) to determine the physical characteristics of each formulation.

2.2.3 Surfactant concentration

Surfactants or surfactant and co-surfactant combinations are certain compounds that are used as emulsifiers at variable concentrations. Based on our lab previous reports, initial surfactant and co-surfactant concentration screening was undertaken with various combinations of Poloxamer 188 and Tween 80.[43] Poloxamer 188 (0.2% w/v) and two concentration levels of Tween 80 (0.75 and 2.0% w/v) were chosen to prepare the NE placebo formulations. In IIG database, Poloxamer 188 is approved up to 0.2% w/v for intramuscular injection and Tween 80 is up to 4% w/w for ophthalmic emulsion, respectively.[45] These formulations were evaluated for physical characteristics.

2.2.4 Preparation of PFD-NE formulations

PFD-NE formulations were prepared by homogenization followed by probe sonication method. The composition of ingredients was listed in Table 2 and Table 3. PFD was accurately weighed and added to oil to obtain a clear liquid and preheated to 70°C in a water bath. At the same time an aqueous phase comprising Poloxamer 188, Tween 80, and Glycerin was mixed in double distilled water and heated to 70 °C. Under continuous mixing, the hot aqueous phase was added to the warm lipid phase to form a coarse emulsion. At 11,000 rpm, the coarse emulsion was then homogenized 5 minutes at 65 °C (T 25 digital Ultra-Turrax IKA, Germany) to form a fine emulsion.

The fine emulsion was gradually cooled down to 25 °C before being placed in an ice bath and ultra-sonic (SONICS® Vibra-Cell™, Newtown, CT, USA) by using a 3mm stepped microtip probe (40% amplitude; Pulse on: 10 seconds, Pulse off: 15 seconds; Time: 10 minutes).

2.2.5 Preparation of PFD solution (PFD-C)

PFD control group (PFD-C) was prepared by accurately weighing PFD then adding PFD and isotonic phosphate buffer saline (IPBS, pH 7.4) in a volume flask to obtain the 1 mg/mL concentration solution.

Table 2: Composition of placebo NE formulations

Batch	Ingredients (% w/v)				
	PFD	**Castor Oil**	**Sesame Oil**	**Soybean Oil**	**Tween®80**
PF-00-NE-P	-	5	-	-	0.75
PF-01-NE-P	-	-	5	-	0.75
PF-02-NE-P	-	-	-	5	0.75
PF-03-NE-P	-	-	5	-	2
PF-04-NE-P	-	-	-	5	2

Each formulation contains 0.2% w/v of poloxamer 188, 2.25% w/v of glycerin and batch size of 10 mL.

Table 3: Composition of PFD-NE formulations

Batch	Ingredients (% w/v)				
	PFD	**Castor Oil**	**Sesame Oil**	**Soybean Oil**	**Tween®80**
PF-00-NE	-	5	-	-	0.75
PF-01-NE	0.1	-	5	-	0.75
PF-02-NE	0.1	-	-	5	0.75
PF-03-NE	0.1	-	5	-	2
PF-04-NE	0.1	-	-	5	2
PF-05-NE	0.5	-	5	-	0.75
PF-06-NE	0.5	-	-	5	0.75
PF-07-NE	0.5	-	5	-	2
PF-08-NE	0.5	-	-	5	2

Each formulation contains 0.2% w/v of poloxamer 188, 2.25% w/v of glycerin and batch size of 10 mL.

2.2.6 Characterization of PFD-NE formulations

Measurement of particle size, polydispersity index (PDI) and zeta Potential (ZP)

The particle size, PDI, and ZP of the placebo and PFD-NE formulations prepared were determined by using a Zetasizer Nano ZS Zen3600 (Malvern Instruments, Westborough, MA, USA); a photon correlation spectroscopy device; at 25 °C in a clear, disposable folded capillary cells. The measurements were attained using a helium-neon laser based on which the data was analyzed as per the volume distribution. The samples were diluted 100 times with bi-distilled water prior to measurements and measured for particle size and zeta potential in triplicate.

Drug content (Assay) of PFD-NE

PFD was extracted from the NE formulations with ACN as extracting solvent. Fifty microliters of PFD-NE formulation were placed in 5 mL volumetric flasks and the volume was made up to 5 mL with ACN. The flasks were vortexed and then sonicated for 15 minutes. The sample was then centrifuged for 10 minutes at 13,300 rpm, in 25℃ (accuSpin Micro 17R, Thermofisher, Germany). The supernatant was further diluted with ACN and analyzed for PFD content using HPLC.

Physical stability

The stability of selected PFD-NE formulations upon storage was evaluated in closed glass vials (VWR® Scintillation Vials, Borosilicate Glass, with Screw Caps) at 4°C and 25°C. The physicochemical characteristics including assay, particle size, PDI, and ZP were evaluated every week.

In-vitro release study

The in-vitro release study of optimized PFD-NE was evaluated for 6 h by the dialysis method, using 10kDa Slide-A-Lyzer™ dialysis devices. Prior to the study, cassettes

were soaked IPBS (20 mL; pH=7.4) overnight at room temperature. The membrane cassettes were placed on scintillation vials containing IPBS (20 mL; pH = 7.4) and maintained in static conditions at 600 rpm under multi-stationed Magnetic Stirrer (IKA, USA). The temperature was then maintained at 34 ± 1°C throughout the study. PFD-NE formulations stored after 1 month were used for in-vitro studies. In the membrane cassettes, 200 µL of PFD-NE and freshly prepared PFD-C were placed in triplicate. Then 1 mL of aliquot was taken at the chosen interval and fresh IPBS were added to maintain the persistent volume of the system. The PFD drug release was analyzed with HPLC as the method mentioned above. The data were analyzed to determine coefficient (r^2) correlation and release kinetics using different mathematical models.[46]

a. Zero order model $Q = Q_0 + kt$

b. First order model $Q = Q_0 * e^{kt}$

c. Higuchi model $Q = k * t^{0.5}$

d. Korsmeyer–Peppas model $Q = k * t^n$

which Q is quantity of drug released in time t, Q_0 is the initial value of Q at zero-time, k is the rate constant, n is the diffusional exponent, a is the time constant and b is the shape parameter. The correlation coefficient (r^2) and the order of release pattern was calculated in each case.

Chapter 3 Results & Discussion

3.1 Effect of oils, surfactants and drug loading on PFD-NE formulation development

Table 4 displays the physical properties of the NE placebo formulations prepared with different concentrations of surfactant and oils. The composition of NE placebos was prepared as described in Table1 but without PFD. The placebos prepared with 5% w/v of castor oil had higher particle size, which is nearly 1000nm. Smaller particle size increases the stability of the NE delivery system, avoiding the formation of aggregates.[47] Furthermore, particle size smaller than 200nm can be easily sterilized by filtration, which is essential for ophthalmic dosage, so it was too large for topical administration.[48] On the other hand, 5% w/v sesame oil and soybean oil, had an average particle size around 200-300 nm, and ZP was between -20 to -30 mV. Furthermore, when the Tween 80 concentration increased from 0.75% w/v to 2 % w/v, particle size was increased. After 7 days, placebos prepared with 5% w/v of sesame oil and soybean oil with two concentration levels of Tween 80 remained constant in particle size, PDI and ZP. This resulted in all subsequent experiments using sesame oil and soybean oil of 5 % w/v and two concentration level of Tween 80 (0.75 and 2% w/v).

As show in Table 5 initially 0.1%w/v drug load was selected since previous literature showed PFD had an anti-fibrotic effect in rabbit eye at 5 mg/mL[36], with

Tween 80 concentration at a lower level (0.75% w/v). Then, the drug load was increased from 0.1% w/v to 0.5 %w/v and the Tween 80 concentration from 0.75% w/v to 2 % w/v. It was observed that different drug loading did not show significant change in the particle size, PDI, ZP, and assay. However, when the Tween 80 concentration was 2.0% w/v, the particle size increased. Meanwhile the PDI, ZP, and Assay did not show significant change in comparison to PFD-NE formulation prepared with 0.75% w/v Tween 80. The particle size increasing could be attribute to the aqueous phase remaining the same for all levels, which allowed placebos with a higher oil concentration to accumulate, resulting in larger particle size. The PDI value of below 0.5 indicates homogenous, uniformly sized vesicles. The PDI of each formulation ranged from 0.17-0.24, which demonstrated uniform and homogenous. ZP value is based on the classical two double layer theory, usually the value between ± 20-30mV demonstrate proper repulsion forces between similar charged particles, thereby reducing flocculation or aggregation and potentially stabilizes the dispersion. The ZP results of the PFD-NEs signified that the components of the formulation have no influence in current experimental conditions. Based on the physiochemical properties, PF-01-NE and PF-02-NE was selected for further investigation.

Table 4: Physical characteristics of various oil concentrations and surfactants on NE placebo formulations at room temperature (mean ± SD, n=3)

Batch	Day 1			Day 7		
	Size (nm)	**PDI**	**ZP (mV)**	**Size (nm)**	**PDI**	**ZP (mV)**
PF-00-NE-P	988.7±114	0.71±0.16	-24.1±1.9	Size too large		
PF-01-NE-P	222.7±3.0	0.24±0.02	-20.6±0.7	216.0±3.1	0.21±0.04	-22.0±0.1
PF-02-NE-P	222.6±4.2	0.22±0.02	-22.3±0.4	210.3±3.1	0.13±0.00	-24.0±0.6
PF-03-NE-P	293.3±8.9	0.15±0.08	-25.6±0.3	289.8±9.3	0.13±0.07	-27.0±0.6
PF-04-NE-P	278.8±13.9	0.19±0.04	-25.4±0.2	258.6±4.0	0.16±0.05	-24.6±0.3

Figure 1 Physical characteristics of various oil concentrations and surfactants on NE placebo formulations

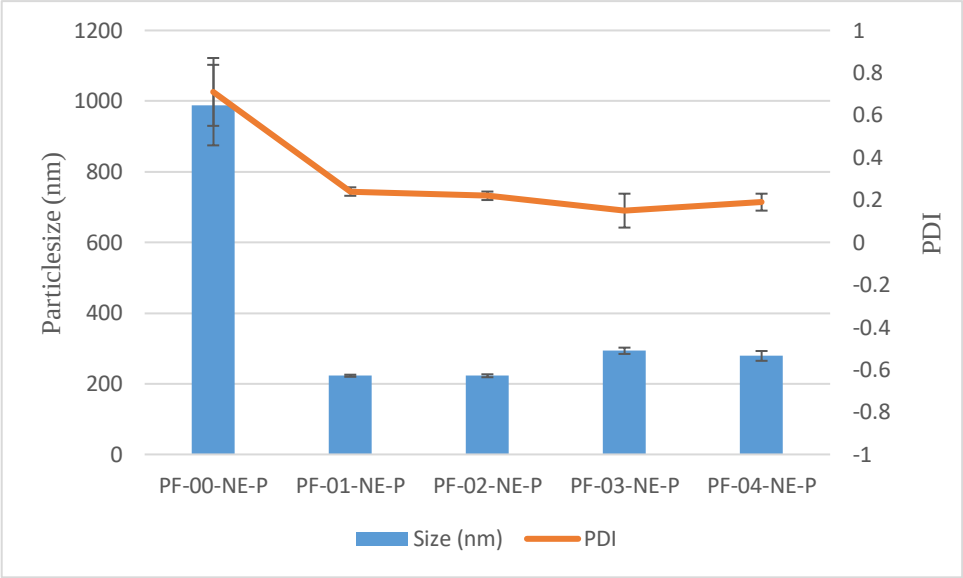

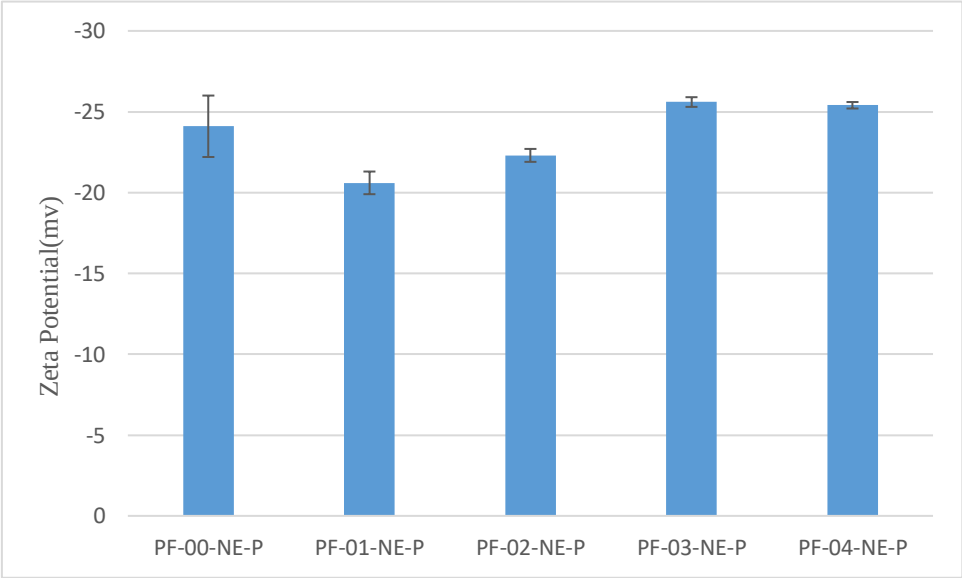

Table 5: Effect of drug loading and surfactant concentration on physicochemical characteristics of PFD-NE formulations (mean ± SD, n=3)

Formulation	Size (nm)	PDI	ZP (mV)	Assay (%)
PF-01-NE	210.6±4.2	0.24±0.01	-24.5±0.2	95.5±7.1
PF-02-NE	227.2±1.0	0.22±0.01	-22.2±0.3	95.4±0.0
PF-03-NE	276.1±10.7	0.21±0.03	-29.1±0.3	105.0±0.3
PF-04-NE	271.6±3.1	0.24±0.04	-24.7±0.2	115.2±0.2
PF-05-NE	212.9±3.0	0.24±0.01	-20.7±0.2	108.3±0.6
PF-06-NE	225.5±5.1	0.18±0.06	-21.8±0.4	107.6±0.5
PF-07-NE	269.6±5.0	0.17±0.0	-24.7±0.6	96.6±0.4
PF-08-NE	264.8±5.8	0.18±0.0	-26.8±0.3	105.7±0.1

Figure 2: Effect of drug loading and surfactant concentration on physicochemical characteristics of PFD-NE formulations

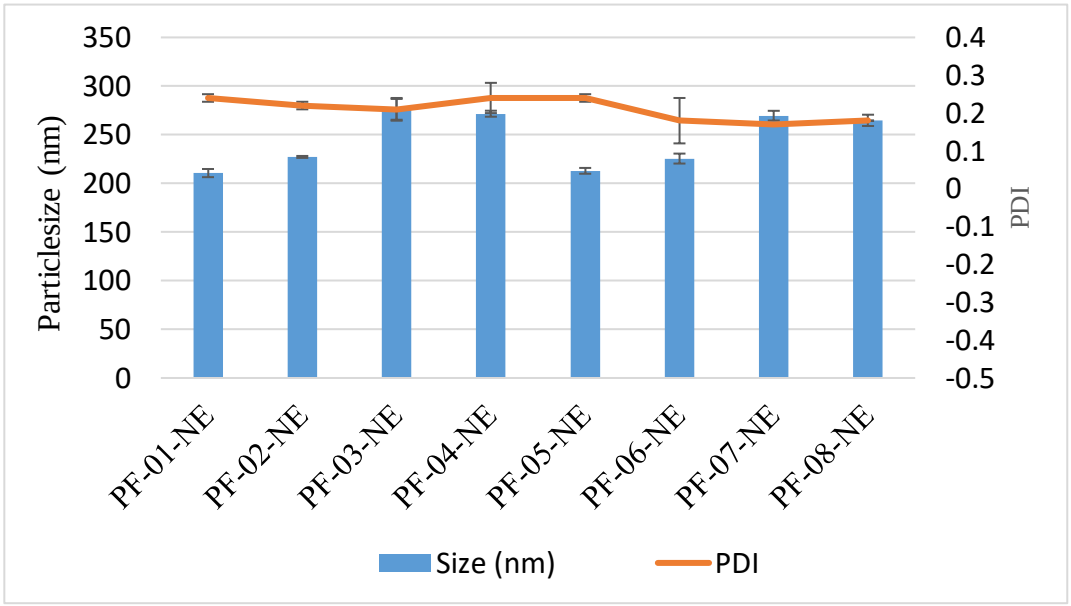

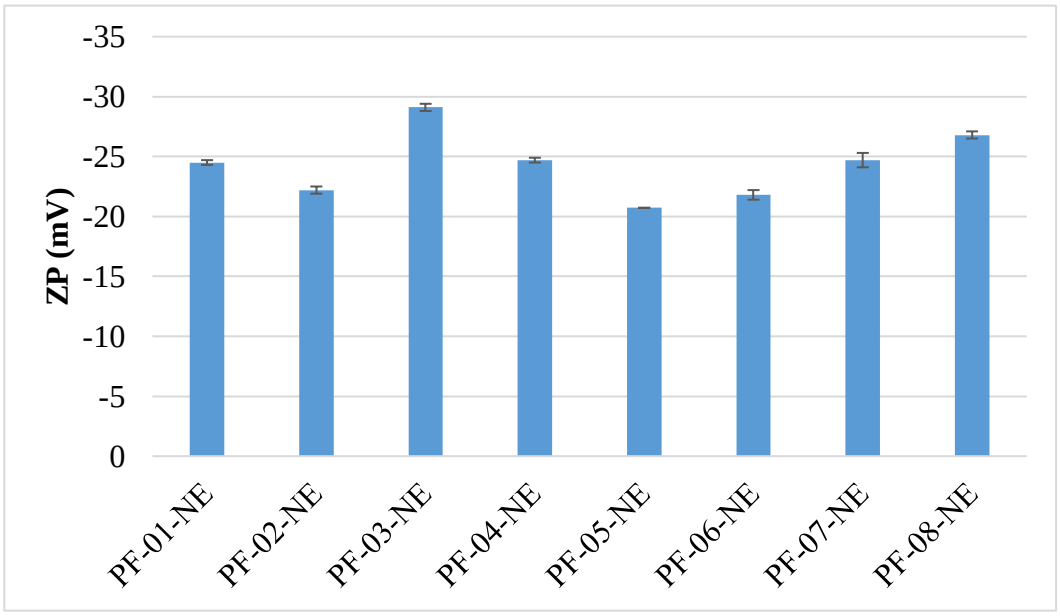

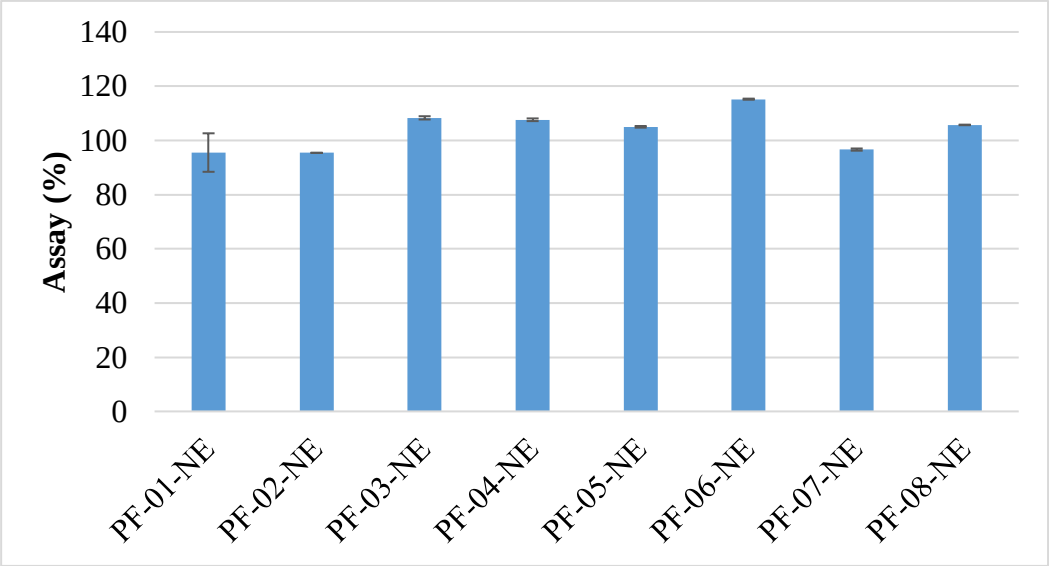

3.2 Physical and chemical stability assessment

Stability studies were carried to determine the influence of various excipients on the drug concentration in PFD-NE and also to determine physicochemical characteristics of the drug product during storage. The particle size, PDI, ZP and Assay were observed after one month at 4℃ and 25℃. The PFD-NEs were found to be a transparent biphasic solution and exhibited no coagulation, aggregation or precipitation after 1 month. The physical characteristics of PF-01-NE and PF-02-NE are presented in Table 8. Both PF-01-NE and PF-02-NE did not show a significant difference on the particle size, PDI, ZP and Assay in different store conditions (4 ℃, 25℃) after 1 month.

Table 6: Particle size, PDI, ZP and assay of PF-01-NE and PF-02-NE formulations stored at conditions of 4 °C and 25 °C (1 month)

Stored condition	Physicochemical Properties	Formulation			
		PF-01-NE		PF-02-NE	
		Duration (days)			
		1	30	1	30
4°C	Size (nm)	203.7±1.0	212.4±1.3	222.0±3.0	225.2±4.5
	PDI	0.25±0.0	0.19±0.0	0.22±0.0	0.16±0.1
	ZP (mv)	-19.2±0.7	-27.1±0.9	-26.3±0.3	-27.8±0.6
	Assay (%)	102.4±1.4	96.9±2.2	107.4±5.0	97.6±0.4
25°C	Size	210.6±4.2	216.0±3.5	227.2±1.0	224.7±5.1
	PDI	0.24±0.01	0.19±0.01	0.22±0.01	0.16±0.01
	ZP	-24.5±0.2	-23.5±0.3	-22.2±0.3	-20.9±1.1
	Assay (%)	95.5±7.1	97.8±1.4	95.4±0.0	99.3±0.4

Figure 3 Particle size, PDI, ZP and assay of PF-01-NE and PF-02-NE formulations stored at different conditions within 1 month

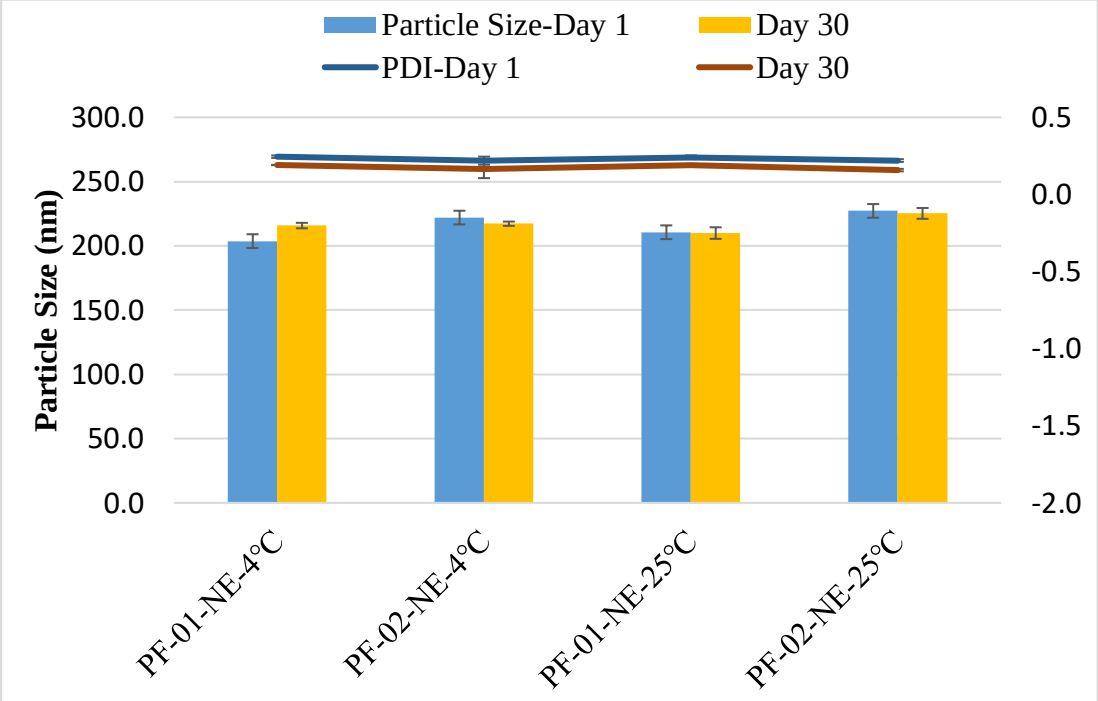

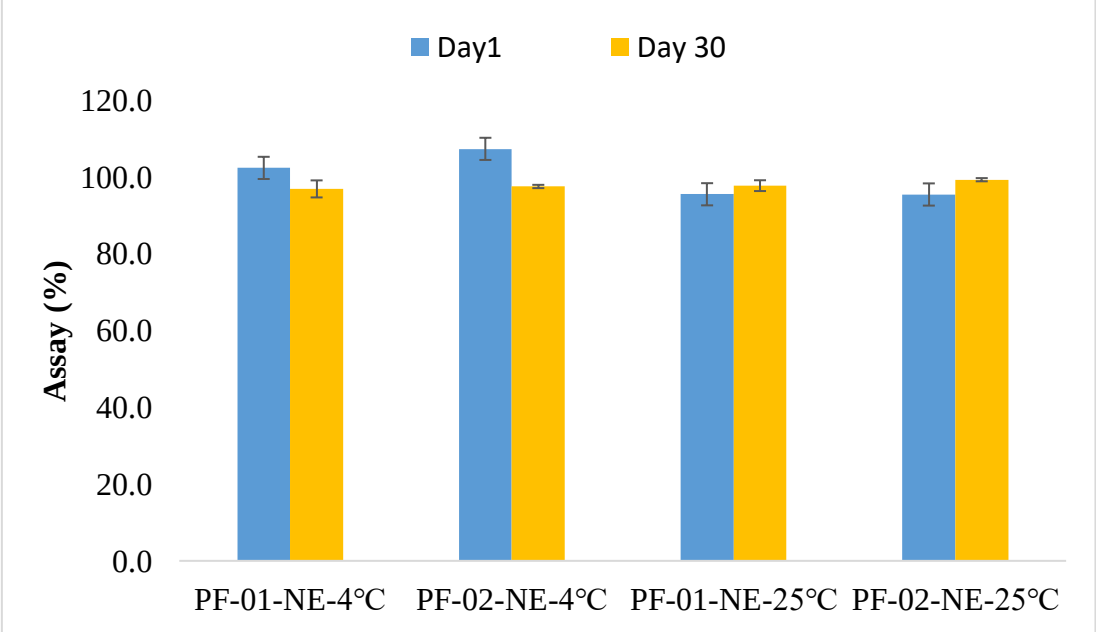

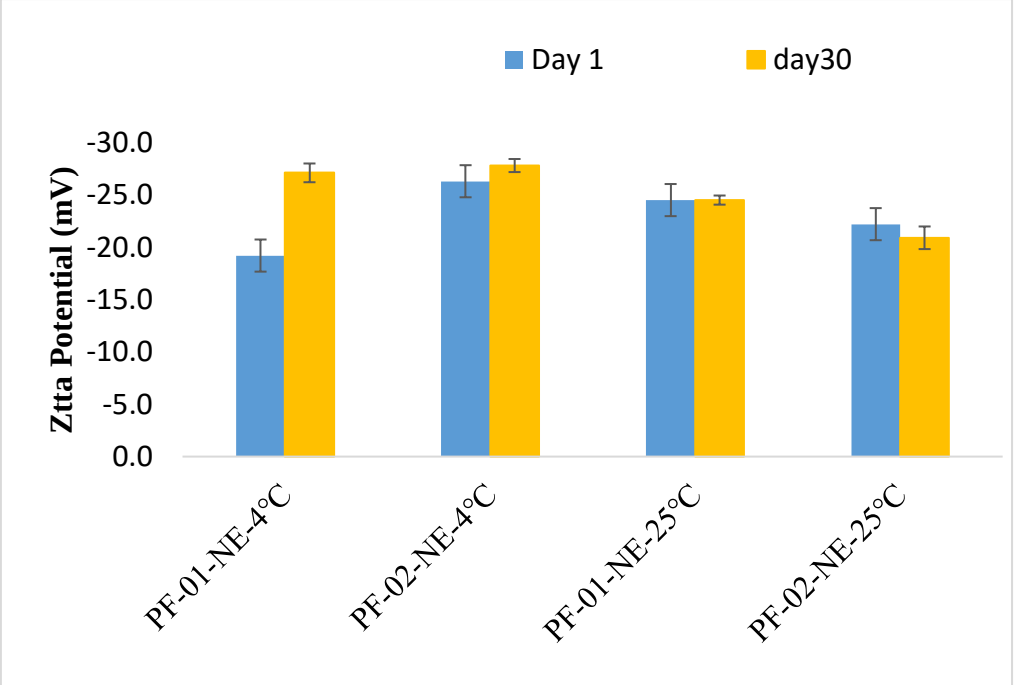

3.3 In-vitro release

The in-vitro release studies were designed to mimic the in-vivo behavior of the formulations. In the present work, to mimic tear fluid, in-vitro release experiments were performed at pH 7.4. The release percentage of PFD at periodic time intervals from PF-01-NE and PF-02-NE after 1 month in comparison with PFD-C formulation shown is in Table 7 and Figure 4. The PFD-C formulation was observed to have a complete release within 4 h while PFD-NE formulations showed complete drug release within 6 h, indicating a sustained release profile compared with PFD-C formulation. The release mechanism for each formulation was studied by various models and the results are summarized in Table 8. The modeling results demonstrate that the kinetics of PFD-NE formulations better fit the Korsmeyer-Peppas model while PFD-C formulation better fit the First order model (r^2=0.993). Drug release following the Korsemeyer-Peppas model means a number of synchronized steps

usually occur that are expected for modified dosage form including diffusion of water and the coupling of the active ingredient diffusion and the oil.

Table 7: *In vitro* release profile of PF-01-NE and PF-02-NE formulations stored at conditions of 4 °C and 25 °C (1month), PFD-C formulation (mean ± SD, n = 3)

Time (h)	Drug release (%)				
		Stored at 4℃		Stored at 25℃	
	PFD-C	PF-01-NE	PF-02-NE	PF-01-NE	PF-02-NE
0.5	39.5±1.7	29.4±2.6	29.8±0.9	29.7±1.5	30.6±0.7
1	57.2±1.7	40.7±3.0	39.9±1.5	40.2±0.8	42.3±2.7
2	76.2±1.1	56.5±2.6	56.1±0.9	57.4±1.9	57.7±3.6
4	86.3±1.3	73.3±2.1	73.5±1.6	72.4±2.4	76.5±2.1
6	84.1±1.0	78.5±1.8	80.2±2.7	78.4±2.7	81.6±1.4

Table 8: Coefficient Relationship (r^2) of model fitting for PFD-NE and PFD-C formulations

Model Name	PFD-C	PF-01-NE	PF-02-NE	PF-01-NE	PF-02-NE
		Stored at 4℃		Stored at 25℃	
Zero order	0.7016	0.9008	0.8938	0.8989	0.9067
First order	0.9932	0.9748	0.9679	0.9752	0.9710
Higuchi	0.8259	0.9696	0.9797	0.9684	0.9723
Korsmeyer-Peppas	0.8781	0.9804	0.9872	0.9797	0.9820

Figure 4: In-vitro release vs time profiles of PF-01-NE and PF-02-NE formulations stored at conditions of 4 °C and 25 °C (1month), PFD-C formulation

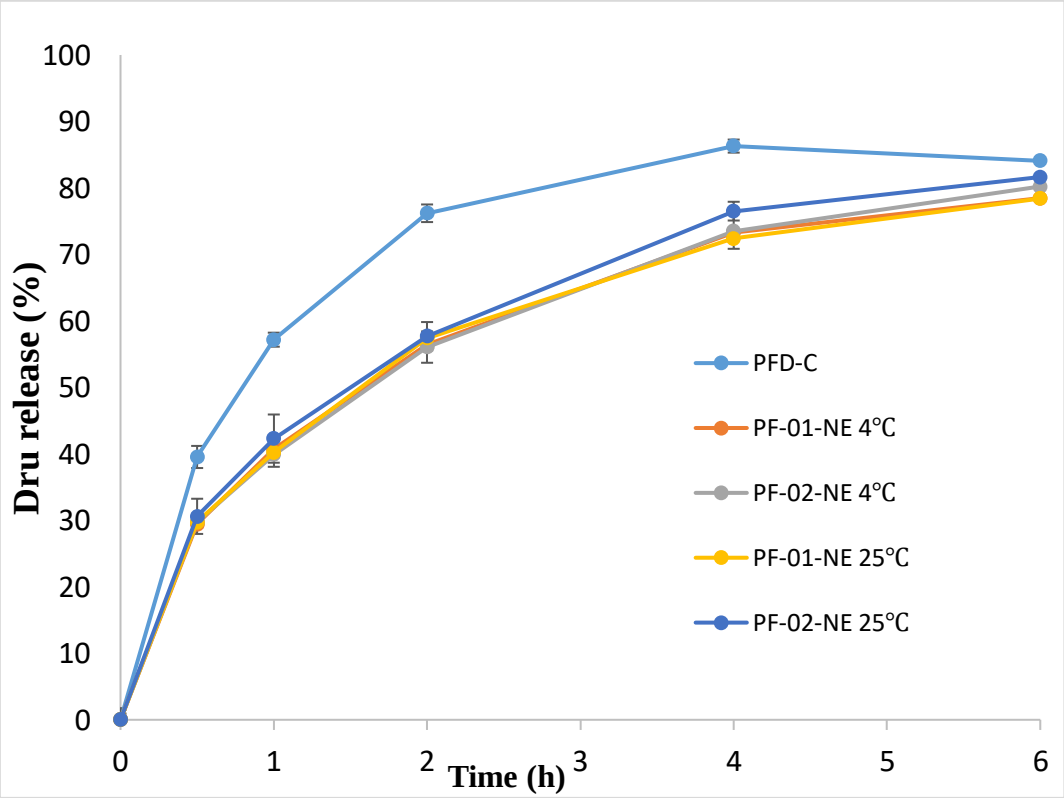

Chapter 4 Conclusion

The NE formulation of PFD were successfully formulated and optimized using soybean oil and sesame oil as oil components, Tween 80 and poloxamer 188 as surfactants. and glycerin as co surfactants, respectively. Optimized NE formulation showed desirable physical characteristics with 100 ± 5% drug content (Assay%). Selected PFD-NE formulations were stable at 4 ℃ and 25 ℃ for one month. The *in vitro* release study revealed the sustain release of PFD in the NE formulation, compared to PFD solution used a control formulation. Further studies include optimize the stability of the formulations for a longer duration of time and in-vitro transcorneal study to confirm the permeability of the formulation.

List of References

1. Rüfer, F.; Schröder, A.; Erb, C. J. C., White-to-white corneal diameter: normal values in healthy humans obtained with the Orbscan II topography system. **2005,** *24* (3), 259-261.
2. Di Girolamo, N.; Bobba, S.; Raviraj, V.; Delic, N. C.; Slapetova, I.; Nicovich, P. R.; Halliday, G. M.; Wakefield, D.; Whan, R.; Lyons, J. G., Tracing the fate of limbal epithelial progenitor cells in the murine cornea. *Stem Cells* **2015,** *33* (1), 157-69.
3. Yu, F. S.; Yin, J.; Xu, K.; Huang, J., Growth factors and corneal epithelial wound healing. *Brain Res Bull* **2010,** *81* (2-3), 229-35.
4. Chang, J.-H.; Huang, Y.-H.; Cunningham, C. M.; Han, K.-Y.; Chang, M.; Seiki, M.; Zhou, Z.; Azar, D. T. J. S. o. o., Matrix metalloproteinase 14 modulates signal transduction and angiogenesis in the cornea. **2016,** *61* (4), 478-497.
5. Kaur, H.; Chaurasia, S. S.; Agrawal, V.; Suto, C.; Wilson, S. E., Corneal myofibroblast viability: opposing effects of IL-1 and TGF beta1. *Exp Eye Res* **2009,** *89* (2), 152-8.
6. Li, W.; Hayashida, Y.; Chen, Y.-T.; Tseng, S. C. J. C. r., Niche regulation of corneal epithelial stem cells at the limbus. **2007,** *17* (1), 26-36.
7. Zhang, Y.; Akhtar, R. A. J. I. o.; science, v., Epidermal growth factor stimulation of phosphatidylinositol 3-kinase during wound closure in rabbit corneal epithelial cells. **1997,** *38* (6), 1139-1148.
8. Hong, J.-W.; Liu, J. J.; Lee, J.-S.; Mohan, R. R.; Mohan, R. R.; Woods, D. J.; He, Y.-G.; Wilson, S. E. J. I. o.; science, v., Proinflammatory chemokine induction in keratocytes and inflammatory cell infiltration into the cornea. **2001,** *42* (12), 2795-2803.
9. Wilson, S. E.; Schultz, G. S.; Chegini, N.; Weng, J.; He, Y.-G. J. E. e. r., Epidermal growth factor, transforming growth factor alpha, transforming growth factor beta, acidic fibroblast growth factor, basic fibroblast growth factor, and interleukin-1 proteins in the cornea. **1994,** *59* (1), 63-72.
10. Nishida, K.; Kinoshita, S.; Yokoi, N.; Kaneda, M.; Hashimoto, K.; Yamamoto, S. J. I. o.; science, v., Immunohistochemical localization of transforming growth factor-beta 1,-beta 2, and-beta 3 latency-associated peptide in human cornea. **1994,** *35* (8), 3289-3294.
11. Moustakas, A.; Heldin, C.-H. J. D., The regulation of TGFβ signal transduction. **2009,** *136* (22), 3699-3714.
12. Saika, S.; Okada, Y.; Miyamoto, T.; Yamanaka, O.; Ohnishi, Y.; Ooshima, A.; Liu, C.-Y.; Weng, D.; Kao, W. W.-Y. J. I. o.; science, v., Role of p38 MAP kinase in regulation of cell migration and proliferation in healing corneal epithelium. **2004,** *45* (1), 100-109.
13. Bhowmick, N. A.; Zent, R.; Ghiassi, M.; McDonnell, M.; Moses, H. L. J. J. o. B. C., Integrin β1 signaling is necessary for transforming growth factor-β activation of p38MAPK and epithelial plasticity. **2001,** *276* (50), 46707-46713.

14. Terai, K.; Call, M. K.; Liu, H.; Saika, S.; Liu, C.-Y.; Hayashi, Y.; Chikama, T.-I.; Zhang, J.; Terai, N.; Kao, C. W.-C. J. I. o.; science, v., Crosstalk between TGF-β and MAPK signaling during corneal wound healing. **2011,** *52* (11), 8208-8215.
15. Marcelo V. Netto, R. R. M., Renato Ambro´sio, Jr., Audrey E. K. Hutcheon, James D. Zieske, Steven E. Wilson, , Wound Healing in the CorneaA Review of Refractive Surgery Complications and New Prospects for Therapy. *Cornea* **2005,** *24* (5), 509-522.
16. Maycock, N. J.; Marshall, J. J. A. o., Genomics of corneal wound healing: a review of the literature. **2014,** *92* (3), e170-e184.
17. MOHAN, R. R.; LIANG, Q.; KIM, W.-J.; HELENA, M. C.; BAERVELDT, F.; WILSON, S. E. J. E. e. r., Apoptosis in the cornea: further characterization of Fas/Fas ligand system. **1997,** *65* (4), 575-589.
18. Jester, J. V.; Moller-Pedersen, T.; Huang, J.; Sax, C. M.; Kays, W. T.; Cavangh, H. D.; Petroll, W. M.; Piatigorsky, J. J. J. o. c. s., The cellular basis of corneal transparency: evidence for 'corneal crystallins'. **1999,** *112* (5), 613-622.
19. Tandon, A.; Tovey, J. C.; Sharma, A.; Gupta, R.; Mohan, R. R. J. C. m. m., Role of transforming growth factor Beta in corneal function, biology and pathology. **2010,** *10* (6), 565-578.
20. Jester, J. V.; Ho-Chang, J. J. E. e. r., Modulation of cultured corneal keratocyte phenotype by growth factors/cytokines control in vitro contractility and extracellular matrix contraction. **2003,** *77* (5), 581-592.
21. Jester, J. V.; Petroll, W. M.; Barry, P. A.; Cavanagh, H. D. J. I. o.; science, v., Expression of alpha-smooth muscle (alpha-SM) actin during corneal stromal wound healing. **1995,** *36* (5), 809-819.
22. Löbler, M.; Buß, D.; Kastner, C.; Mostertz, J.; Homuth, G.; Ernst, M.; Guthoff, R.; Wree, A.; Stahnke, T.; Fuellen, G. J. M. v., Ocular fibroblast types differ in their mRNA profiles—implications for fibrosis prevention after aqueous shunt implantation. **2013,** *19*, 1321.
23. Guo, X.; Yang, Y.; Liu, L.; Liu, X.; Xu, J.; Wu, K.; Yu, M., Pirfenidone Induces G1 Arrest in Human Tenon's Fibroblasts In Vitro Involving AKT and MAPK Signaling Pathways. *J Ocul Pharmacol Ther* **2017,** *33* (5), 366-374.
24. Comstock, T. L.; Sheppard, J. D. J. E. o. o. p., Loteprednol etabonate for inflammatory conditions of the anterior segment of the eye: twenty years of clinical experience with a retrometabolically designed corticosteroid. **2018,** *19* (4), 337-353.
25. Dupps Jr, W. J.; Wilson, S. E. J. E. e. r., Biomechanics and wound healing in the cornea. **2006,** *83* (4), 709-720.
26. Taniguchi, H.; Ebina, M.; Kondoh, Y.; Ogura, T.; Azuma, A.; Suga, M.; Taguchi, Y.; Takahashi, H.; Nakata, K.; Sato, A.; Takeuchi, M.; Raghu, G.; Kudoh, S.; Nukiwa, T.; Pirfenidone Clinical Study Group in, J., Pirfenidone in idiopathic pulmonary fibrosis. *Eur Respir J* **2010,** *35* (4), 821-9.
27. Antonio Di Sario, E. B., Gianluca Svegliati Baroni, Francesco Ridolfi,Alessandro Casini, Elisabetta Ceni, Stefania Saccomanno, Marco Marzioni, Luciano Trozzi, Paola Sterpetti, Silvia Taffetani, Antonio Benedetti, Effect of pirfenidone on rat hepatic

stellate cell proliferation and collagen production. *Journal of Hepatology* **2002,** *37*, 584–591.
28. Azuma, A.; Nukiwa, T.; Tsuboi, E.; Suga, M.; Abe, S.; Nakata, K.; Taguchi, Y.; Nagai, S.; Itoh, H.; Ohi, M.; Sato, A.; Kudoh, S., Double-blind, placebo-controlled trial of pirfenidone in patients with idiopathic pulmonary fibrosis. *Am J Respir Crit Care Med* **2005,** *171* (9), 1040-7.
29. Raghu, G.; Craig Johnson, W.; Lockhart, D.; Mageto, Y. J. A. j. o. r.; medicine, c. c., Treatment of idiopathic pulmonary fibrosis with a new antifibrotic agent, pirfenidone: results of a prospective, open-label Phase II study. **1999,** *159* (4), 1061-1069.
30. Hewitson TD, K. K., Tait MG, Martic M, Jones CL, Margolin SB, Becker GJ., Pirfenidone reduces in vitro rat renal fibroblast activation and mitogenesis. *J Nephrol* **2001,** *14*, 453-60.
31. Silva, R. O.; Costa, B. L. D.; Silva, F. R. D.; Silva, C. N. D.; Paiva, M. B.; Dourado, L. F. N.; Malachias, A.; Souza Araujo, A. A.; Nunes, P. S.; Silva-Cunha, A., Treatment for chemical burning using liquid crystalline nanoparticles as an ophthalmic delivery system for pirfenidone. *Int J Pharm* **2019,** *568*, 118466.
32. Lin, X.; Yu, M.; Wu, K.; Yuan, H.; Zhong, H., Effects of pirfenidone on proliferation, migration, and collagen contraction of human Tenon's fibroblasts in vitro. *Invest Ophthalmol Vis Sci* **2009,** *50* (8), 3763-70.
33. Na, J. H.; Sung, K. R.; Shin, J. A.; Moon, J. I., Antifibrotic effects of pirfenidone on Tenon's fibroblasts in glaucomatous eyes: comparison with mitomycin C and 5-fluorouracil. *Graefes Arch Clin Exp Ophthalmol* **2015,** *253* (9), 1537-45.
34. Hisashi Oku, H. N., Tatsuya Horikawa, Yuji Tsuruta, Ryuji Suzuki Pirfenidone suppresses tumor necrosis factor-alpha, enhances interleukin-10 and protects mice from endotoxic shock.pdf. *European Journal of Pharmacology* **2002,** *446*, 167–176.
35. Guoying Sun, X. L., Hua Zhong, Yangfan Yang, Xuan Qiu, Chengtian Ye, Kaili Wu, Minbin Yu, Pharmacokinetics of pirfenidone after topical administration in rabbit eye. *Molecular Vision* **2011,** *17*, 2191-2196.
36. Gaudana, R.; Ananthula, H. K.; Parenky, A.; Mitra, A. K. J. T. A. j., Ocular drug delivery. **2010,** *12* (3), 348-360.
37. Boddu, S. H.; Gunda, S.; Earla, R.; Mitra, A. K. J. B., Ocular microdialysis: a continuous sampling technique to study pharmacokinetics and pharmacodynamics in the eye. **2010,** *2* (3), 487-507.
38. Bachu, R. D.; Chowdhury, P.; Al-Saedi, Z. H.; Karla, P. K.; Boddu, S. H. J. P., Ocular drug delivery barriers—role of nanocarriers in the treatment of anterior segment ocular diseases. **2018,** *10* (1), 28.
39. Patel, A.; Cholkar, K.; Agrahari, V.; Mitra, A. K. J. W. j. o. p., Ocular drug delivery systems: an overview. **2013,** *2* (2), 47.
40. Vandamme, T. F.; Brobeck, L. J. J. o. c. r., Poly (amidoamine) dendrimers as ophthalmic vehicles for ocular delivery of pilocarpine nitrate and tropicamide. **2005,** *102* (1), 23-38.
41. Vandamme, T. F. J. P. i. r.; research, e., Microemulsions as ocular drug delivery systems: recent developments and future challenges. **2002,** *21* (1), 15-34.

42. Gurpreet, K.; Singh, S. J. I. J. o. P. S., Review of nanoemulsion formulation and characterization techniques. **2018,** *80* (5), 781-789.
43. Balguri, S. P.; Adelli, G. R.; Janga, K. Y.; Bhagav, P.; Majumdar, S., Ocular disposition of ciprofloxacin from topical, PEGylated nanostructured lipid carriers: Effect of molecular weight and density of poly (ethylene) glycol. *Int J Pharm* **2017,** *529* (1-2), 32-43.
44. Chen, L.; Weng, Q.; Li, F.; Liu, J.; Zhang, X.; Zhou, Y., Pharmacokinetics and Bioavailability Study of Tubeimoside I in ICR Mice by UPLC-MS/MS. *J Anal Methods Chem* **2018,** *2018*, 9074893.
45. (FDA)，, F. a. D. A. Inactive Ingredient Search for Approved Drug Products. https://www.accessdata.fda.gov/scripts/cder/iig/index.cfm.
46. Costa, P.; Lobo, J. M. S. J. E. j. o. p. s., Modeling and comparison of dissolution profiles. **2001,** *13* (2), 123-133.
47. Heurtault, B.; Saulnier, P.; Pech, B.; Proust, J.-E.; Benoit, J.-P. J. B., Physico-chemical stability of colloidal lipid particles. **2003,** *24* (23), 4283-4300.
48. Mehnert, W.; Mäder, K. J. A. d. d. r., Solid lipid nanoparticles: production, characterization and applications. **2012,** *64*, 83-101.

VITA

Chuntian Cai

EDUCATION

University of Mississippi 2018-Present
Department of Pharmaceutics and Drug Delivery
Master of Science

Chengdu Medical College (Chengdu, China) 2007
Bachelor of Science in Pharmacy

CERTIFICATIONS & HONORS

The Hands-on Course in Tablet Technology 2018

Pharmacist Certificate (Intermediate Level)-Issued by the National Health and Family Planning Commission of P.R.C. 2017

Licensed Pharmacist Certificate-Issued by China Food and Drug Administration 2017

CONVENTION PRESENTATIONS

Chuntian C., Corinne S., Kai-Wei W., Narendar D., Babu T., Soumyajit M. (Oct 2019) *"Design, development and in vitro characterization of a new 8- aminoquinoline derivative loaded solid lipid nanoparticles for relapsing malaria".*
Poster presentation at American Association of Pharmaceutical Scientists Conference (AAPS), San Antonio, Texas